Model. Earth Syst. Environ. (2016) 2:142
DOI 10.1007/s40808-016-0201-z

ORIGINAL ARTICLE

# Seismicity and recent stress regime of Diyala City, Iraq–Iran border

**Wathiq Abdulnaby[1] · Rafed Al-Mohmed[1] · Maher Mahdi[1]**

Received: 15 July 2016 / Accepted: 23 July 2016


**Abstract** Diyala city is one of the most seismically active cities in Iraq. It is located in the northeastern part of Iraq at the Iraq–Iran border. In this study, the seismic history of Diyala during 10 years (2004–2014) has been studied. Three seismic catalogs, which are the EMSC, IRIS, IRSC, were used to study the seismic history of the study area. From the seismic history, six seismic swarms were recognized; these are: January 2005, September 2008, June 2009, August 2009, November 2013, and August 2014. In order to study the stress regime in the study area, focal mechanism solutions of eight earthquakes were collected from the GCMT catalog. Most of the focal mechanism solutions of earthquakes in the study area, that have magnitude 5 and more, indicate reverse movements formed by compressional forces. The study area has faults with different lengths and directions. However, the fault that is responsible of earthquakes with magnitude 5 and more is a reverse fault with strike direction equals 314°, dip direction equals 224°, and dip angle equals 64°. The attitudes of the principal stress axes at that fault surface are: $\sigma_1$ 18°/232°, $\sigma_2$ 10°/139° and $\sigma_3$ 69°/022°. In fact, this fault represents the northwestern part of longer fault, which is Badra-Amarah fault that extends from Amarah city in the southeastern to Mandali city to the northwestern. It is the most seismically active fault in Iraq.

**Keywords** Seismicity of Iraq · Diyala city · Stress analysis · Stress inversions

✉ Maher Mahdi
maher_mandeel@yahoo.com

[1] Seismological Lab, Department of Geology, College of Sciences, University of Basrah, Basra, Iraq

## Introduction

Diyala city is located in the northeastern part of Iraq at the Iraq–Iran border; and it is one of the most seismically active cities in Iraq (Fig. 1). The population of the city is about 1.5 million and its area is about 17.685 km$^2$. Numbers of felt earthquakes occur every year and cause some damages in weak structures.

The aim of this study is to shade light on the seismic history of Diyala city during the last 10 years (from October, 2004 to October, 2014) by using different seismological catalogs. Additionally, focal mechanism solutions of big earthquakes (equal or more than 5 magnitude) in the study area were collected from the Global Centroid-Moment-Tensor (GCMT) catalog in order to depict the slip movement on the active fault or faults in the study area, and then drive the stress regime from the focal mechanism solutions by using two formal stress inversions.

## Seismotectonics setting

Iraq is part of the Alpine-Himalayan minor seismic belt and it is located at the northeastern edge of the Arabian plate. Therefore, the seismicity of Iraq has displays a direct relation with the general trend of the seismicity of the Bitlis–Zagros Fold and Thrust Belt (Abdulnaby et al. 2013, 2014). Linear alignments of epicenters are often correlated with the major trending faults, which have two trends these are: northeast-southwest and northwest-southeast (Jassim and Goff 2006). The depths of earthquakes in general increase toward the Zagros Thrust Zone from southwest to northeastern. The distribution of seismic activity along the Bitlis–Zagros Folded and Thrust Belt is non-homogenous and scattered because the epicenters are

Published online: 28 July 2016

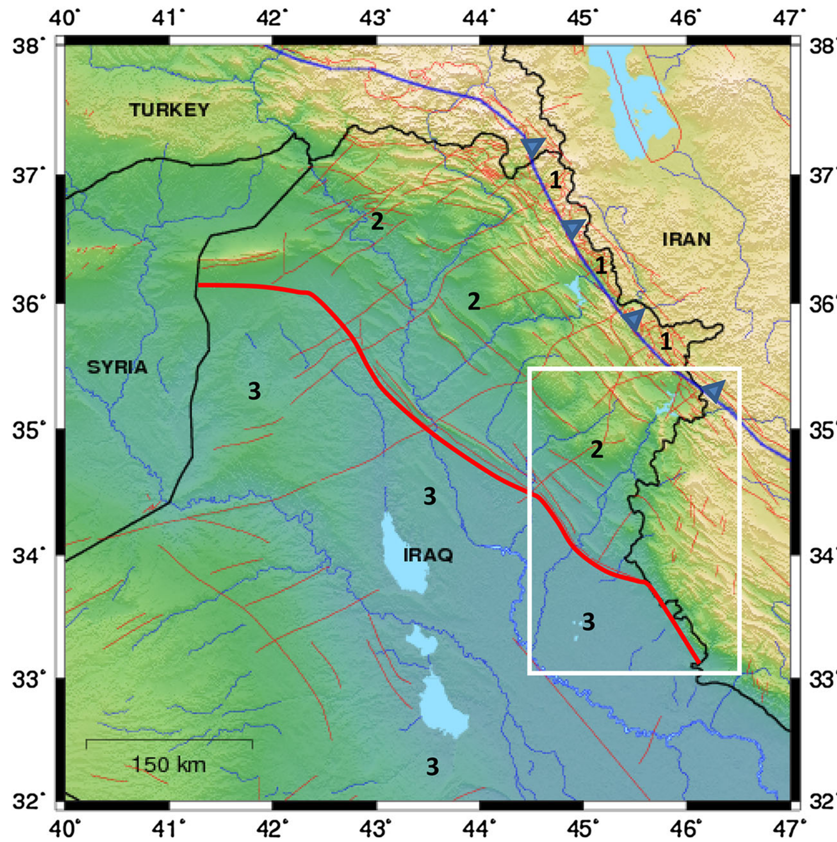


**Fig. 1** Geological map of northern Iraq. *1*, *2*, and *3* are thrust, folded, and unfolded zones, respectively. *Blue line with triangles* is the Zagros suture line. *Red thick line* is the boundary between the folded zone in the north and unfolded zone in the south. *Red thin lines* represent faults in the region taken from Seber et al. (1997). The *white rectangle* represents the study area

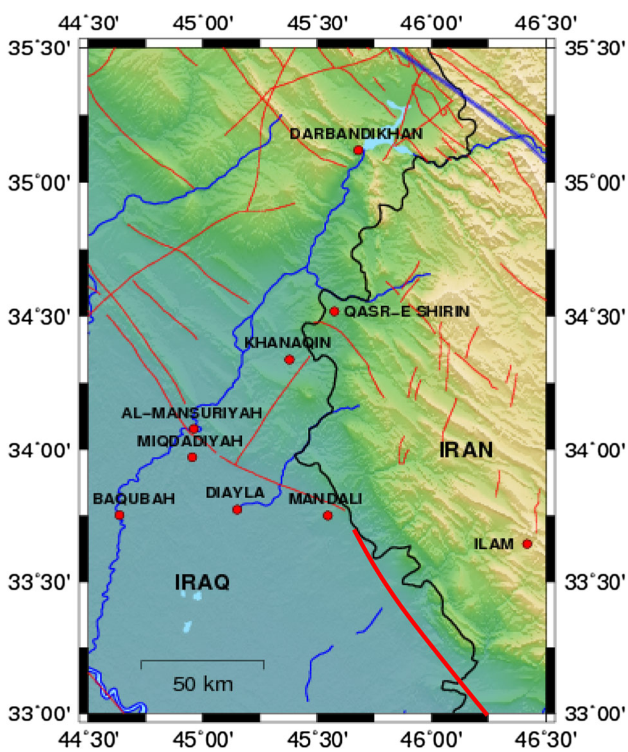


**Fig. 2** Faults in the study area. Faults represented by *thin red lines* are taken from Seber et al. (1997). These faults were diagnosed by satellite images. The *red thick line* is the northern part of the Badra-Amarah fault taken from Abdulnaby et al. (2015)

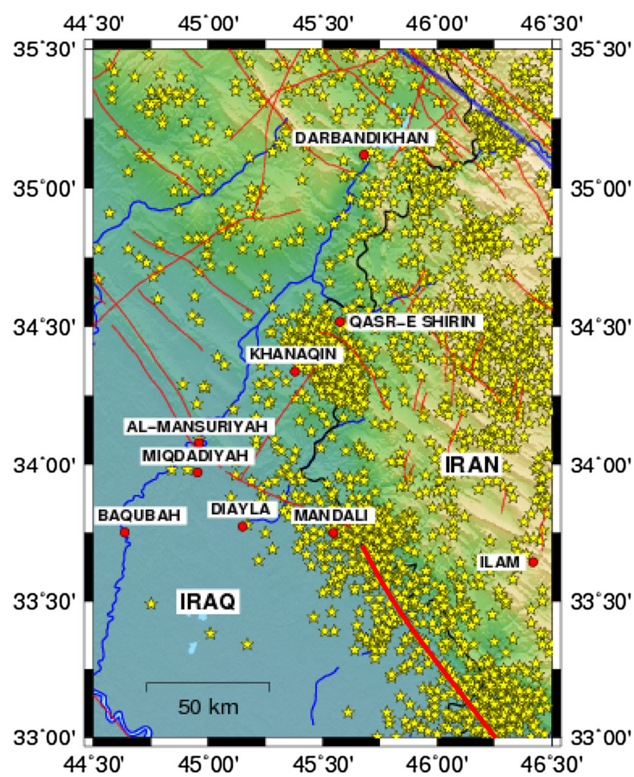


**Fig. 3** Seismicity of study area based on the Iranian Seismologic Center (IRSC) catalog from January, 2006 to October, 2014

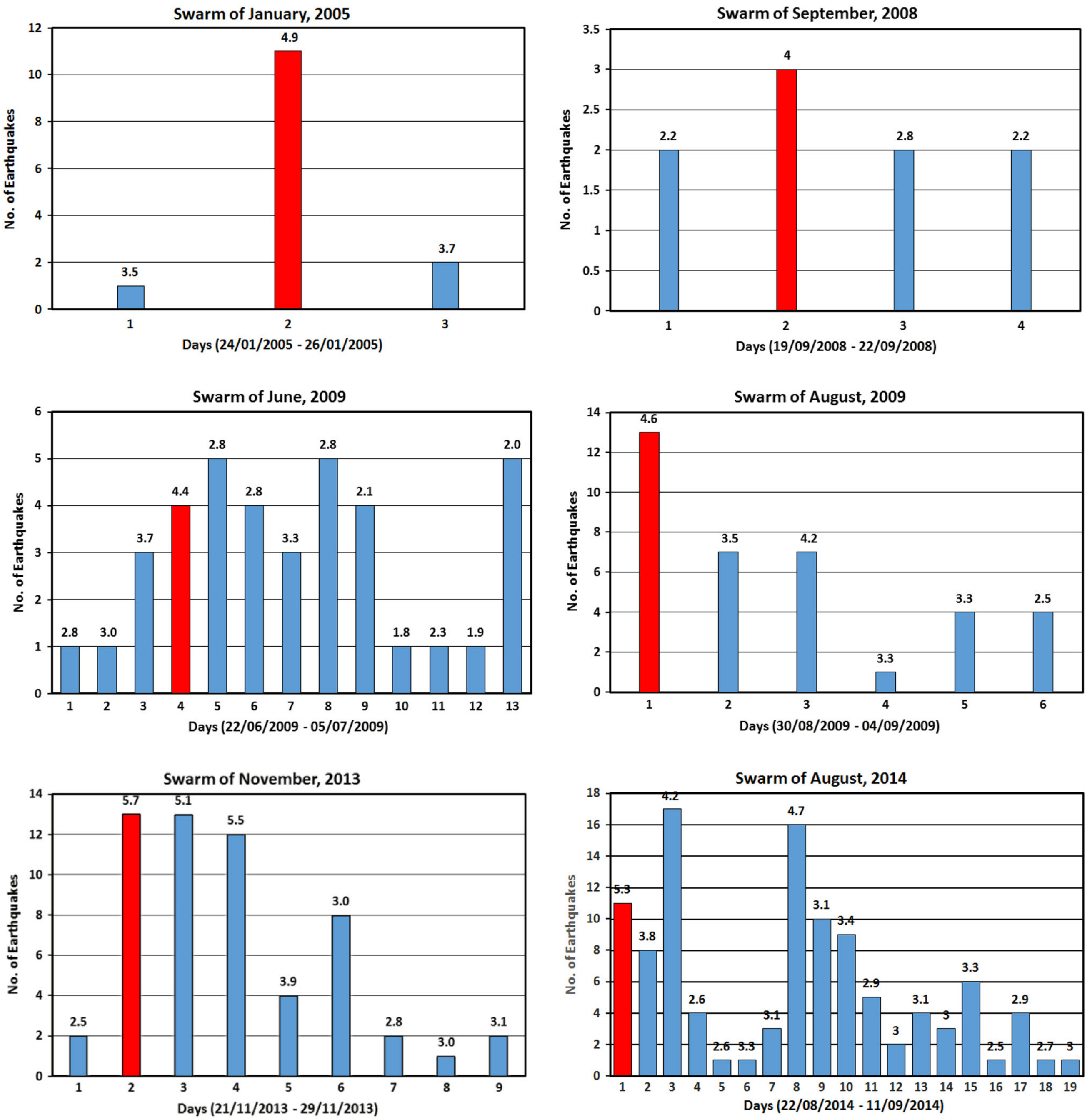


**Fig. 4** Graphical descriptions of the six swarms of Diyala city during 10 years (2004–2014). *Red column* depicts the day of mainshock. *Number above each column* represents the highest magnitude during the day

concentrated in some parts of the belts (Alsinawi 1988). This non-homogeneity may be due to the change in geometry of the Arabian plate edge that is in collision with the Iranian and Turkish plates and due to the rotational movement of the Arabian plate (Numan 1997).

Generally, the tectonics of the study area is controlled by the collision of the Arabian and Iranian plates (Fig. 1). Iraq mainly comprises longitudinal tectonic unites parallel to the Zagros Suture. These units are present in a narrow belt along the Iraq–Iran border in the northeastern Iraq. The northeastern part of the study area is located within the Folded Zone according to Jassim and Goff (2006) and within the Suspended Basin of the Foothill Zone according to Numan (1997). This tectonic zone of Iraq is characterized by folds with long axes with direction NW–SE. These folds are associated with listric faults parallel to their axes (Numan and Al-Azzawi 1993). The southwestern part of the study area is located within the Mesopotamian Zone

**Table 1** Mainshocks of six swarms at Diyala city during 10 years (2004–2014) have taken from different sources

| Date | Origin time (UTC) | Latitude | Longitude | Depth (km) | Magnitude | Network center |
|---|---|---|---|---|---|---|
| 2005/01/25 | 11:39:18.0 | 33.700 | 45.760 | 20 | 5.1 MB | EMSC |
| | 11:39:19.0 | 33.440 | 45.860 | 48.6 | 4.9 MB | IRIS |
| 2008/09/20 | 12:35:13.7 | 33.477 | 45.864 | 4.3 | 4.0 MN | IRSC |
| | 12:35:15.0 | 33.580 | 45.950 | 13 | 4.5 MB | IRIS |
| 2009/06/25 | 15:04:51.9 | 33.010 | 46.340 | 10 | 4.4 MB | EMSC |
| | 15:04:53.7 | 33.102 | 46.341 | 8 | 4.4 MN | IRSC |
| 2009/08/30 | 14:04:37.0 | 33.160 | 46.470 | 15 | 4.7 MB | EMSC |
| | 14:04:34.1 | 33.047 | 46.405 | 10 | 4.6 MN | IRSC |
| 2013/11/22 | 18:30:57.0 | 34.289 | 45.555 | 10 | 5.7 MN | IRSC |
| | 18:31:03.0 | 34.340 | 45.650 | 47.5 | 5.6 MB | IRIS |
| 2014/08/22 | 20:06:05.0 | 33.800 | 45.770 | 20.7 | 5.4 MB | IRIS |
| | 20:06:05.0 | 33.784 | 45.769 | 19.8 | 5.3 MN | IRSC |
| | 20:06:04.0 | 33.630 | 45.720 | 20 | 4.9 MB | EMSC |

according to Jassim and Goff (2006) and within the Sagged Basin of the Mesopotamian Zone according to Numan (1997). Hemrin folds represent the boundary between the northeastern part (Folded Zone) and the southeastern part (Unfolded Zone) of the study area. Within the southeastern part of the study area, no structural features can be seen easily on surface due to the high thickness of Quaternary sediments that range from few meters up to 180 m (Fouad and Sissakian 2011).

## Faults

Diyala city is located within a geological region that has many faults with different lengths and directions. Figure 2 depicts the faults in the study area. The faults that are represented by thin red lines are taken from Seber et al. (1997). These faults were diagnosed by satellite images. Abdulnaby et al. (2015) diagnosed a seismic active fault that is located at the Iraq–Iran border and pass near Amarah city in the south, through Badra city, and then reach Mandali city. This fault is physically a normal fault, but the recent movement on its surface is reverse movement due to the collision between the Arabian and Iranian plates. In Fig. 2, this fault is represented by thick red line.

## Seismic history

The seismic history of Diyala city was studied according to different seismological catalogs, these are: the European-Mediterranean Seismological Centre (EMSC), the Incorporated Research Institutions for Seismology (IRIS), and the Iranian Seismological Center (IRSC). From the spatial distribution of earthquakes in Diyala city, the folded area has the majority of earthquakes, while the unfolded area has fewer earthquakes (Fig. 3). The spatial distribution of epicenters is non-homogenous and scattered. In general, the epicenters are concentrated in an area between Qasr-e Shirin and Khanaqin and along the Iraq–Iran border at the northeastern part of Badra-Amarah fault.

Identifying earthquake swarms is an important step before study the seismic history of the study area. Keilis-Borok et al. (1978) defined a swarm as ‘spatial clustering of earthquakes at a time when the seismicity of the region is above average’. Based on this identification, a swarm must meet criteria in both time and space domains, which must be true simultaneously for a swarm to exist (Michael and Toksoz 1982). Each swarm must have a mainshock, which is the largest earthquake in a sequence. The mainshock sometimes is preceded by one or more foreshocks, and almost always followed by many aftershocks.

**Table 2** Statistical descriptions of six swarms of Diyala city during 10 years (2004–2014)

| Swarm | No. of foreshocks | No. of aftershocks | No. of days |
|---|---|---|---|
| January, 2005 | 1 | 10 | 3 |
| September, 2008 | 2 | 6 | 4 |
| June, 2009 | 5 | 32 | 13 |
| August, 2009 | 0 | 41 | 6 |
| November, 2013 | 2 | 54 | 9 |
| August, 2014 | 0 | 106 | 19 |

**Table 3** Source parameters and focal mechanism solutions of six earthquakes in Diyala city derived from the moment tensor inversion based on the GCMT catalog

| No. | Data | O. time UTC | Lat. | Log. | F.D | Mw | Scalar moment (N m) | Fault plane 1 | | | Fault plane 2 | | | Moment stress axes | | | | | | Horizontal stress axes | | Regime |
|---|---|---|---|---|---|---|---|---|---|---|---|---|---|---|---|---|---|---|---|---|---|---|
| | | | | | | | | S | D | R | S | D | R | P | | N | | T | | $S_{Hmax}$ | $S_{hmin}$ | |
| | | | | | | | | | | | | | | PL | AZ | PL | AZ | PL | AZ | AZ | AZ | Code |
| 1 | 1998-08-05 | 14:27:00.5 | 33.50 | 46.00 | 33.0 | 5.6 | 3.16e+24 | 183 | 20 | 052 | 043 | 74 | 103 | 28 | 123 | 12 | 219 | 59 | 330 | 114 | 024 | TF |
| 2 | 2002-06-18 | 03:19:23.0 | 33.74 | 45.17 | 33.0 | 5.3 | 9.84e+23 | 242 | 74 | 005 | 151 | 85 | 164 | 08 | 198 | 73 | 314 | 15 | 105 | 017 | 107 | SS |
| 3 | 2004-10-16 | 10:04:37.6 | 33.56 | 45.63 | 14.2 | 4.8 | 2.18e+23 | 282 | 42 | 019 | 177 | 77 | 130 | 21 | 238 | 39 | 346 | 43 | 126 | 050 | 140 | UF |
| 4 | 2005-01-25 | 11:39:20.9 | 33.40 | 45.69 | 12.0 | 4.9 | 2.97e+23 | 350 | 27 | 129 | 127 | 70 | 072 | 23 | 231 | 17 | 133 | 61 | 010 | 059 | 149 | TF |
| 5 | 2013-11-22 | 06:51:29.6 | 34.28 | 45.31 | 18.1 | 5.7 | 3.96e+24 | 339 | 24 | 109 | 139 | 68 | 082 | 22 | 235 | 07 | 142 | 66 | 035 | 059 | 149 | TF |
| 6 | 2013-11-22 | 18:31:01.8 | 34.22 | 45.44 | 13.9 | 5.7 | 4.42e+24 | 345 | 35 | 125 | 134 | 62 | 068 | 14 | 236 | 15 | 142 | 69 | 007 | 060 | 150 | TF |
| 7 | 2013-11-24 | 18:05:43.7 | 34.18 | 45.43 | 18.7 | 5.5 | 2.33e+24 | 013 | 41 | 116 | 160 | 54 | 069 | 07 | 265 | 17 | 173 | 72 | 016 | 087 | 177 | TF |
| 8 | 2014-08-22 | 20:06:06.6 | 33.67 | 45.51 | 19.8 | 4.9 | 3.34e+23 | 324 | 33 | 099 | 133 | 57 | 084 | 12 | 227 | 05 | 136 | 77 | 024 | 048 | 138 | TF |

*O. time (UTC)* original time in UTC, *Lat* latitude in degree, *Log* longitude in degree, *D* calculated depth, *Mag* reported magnitude, *S* strike, *D* dip, *R* rake angle, *P*, *N*, and *T* compressional, normal, and tensional moment stress axes, respectively, *PL* plunge angle, *AZ* azimuth

The area had six swarms during the period from 2004 to 2014 (Fig. 4; Tables 1, 2). The first swarm extends only for 3 days from 24-01 to 26-01-2005, and it represents the shorter swarm. The mainshock happened in the second day with magnitude 4.9. The second swarm continues for 4 days from 19-09 to 22-09-2008. The mainshock happened at the second day of the swarm with magnitude 4 and this day had three of earthquakes while the other days had two earthquakes. The third swarm consists of 13 days from 22-06 to 05-07-2006. The mainshock happened in the fourth day with magnitude 4.4. The fourth swarm extends for 6 days from 30-08-2006 to 04-09-2006, and its mainshock was with magnitude 4.6. The fifth swarm occurred at 6 km northeast of the Miqdadiyah city. The swarm started 22 to 29-11-2013, and the mainshock was happened in the second day with magnitude 5.6. The last swarm, which represents the longest swarm, consists of 19 days started from 22-08 to 11-09-2014. The mainshock happened in the first day. The third day represents the most frequent with rate 17 events.

## Focal mechanism solutions

The focal mechanism of an earthquake describes the orientation of the displacement on the fault that generates the seismic waves. Therefore, it is also known as a fault-plane

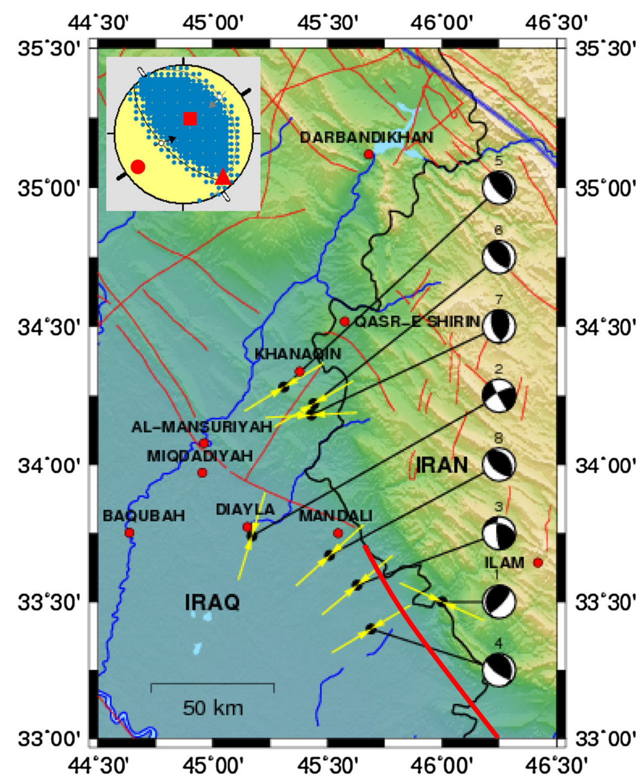


**Fig. 5** Focal mechanism solutions of eight earthquakes in the Diyala area from the GCMT catalog and the maximum horizontal stress axes (*yellow arrows*) based on Table 3. The *panel in the top left* of the map represents the final solution of the focal mechanism solutions in the study area

solution. One of the global institutions that make an effort to determine the focal mechanism solutions for earthquakes with mb magnitudes of 5.0 and greater is the Harvard University (USA) group that estimates the Global Centroid Moment Tensor (GCMT) solutions (Dziewonski et al. 1981; Ekström et al. 2012).Table 3 shows eight focal mechanism solutions in the study area that were calculated from the GCMT. These solutions were plotted on a map as shown in Fig. 5. The solutions indicate that the movement on faults in the study area is a reverse mechanism formed by compressional forces.

## Recent stress analysis

From the eight focal mechanism solutions, two methods of stress inversion were used in order to estimate the directions of the three principal stress axes that effect on faults in Diyala city. These methods are the Improved Right Dihedron and the Rotational Optimization methods. The three principal stress axes are: the maximum stress axis ($\sigma_1$), the intermediate stress axis ($\sigma_2$), and the minimum stress axis ($\sigma_3$). The principal stress axes usually converted to the horizontal stress axes, these are: the maximum horizontal stress axis ($S_H$), the minimum horizontal stress axis ($S_h$), and the vertical stress axis ($S_V$), which are perpendicular to each other. The reason for that converting is to be able to plot the stress directions on a map. The best way to display the tectonic stress is to map the azimuth of the horizontal stress because it is the most dominant stress due to the horizontal plate driving mechanism.

In this study, the Windows version of the TENSOR program (Win-Tensor version 4.0.4) was used to invert the moment stress axes to the principal and horizontal stress axes. This program is free source program developed originally in DOS by Delvaux (1993) and then modified for Windows by Delvaux and Sperner (2003). The graphical output of the stress inversion by the TENSOR program depicts the projection of the principal stress axes in a lower hemisphere equal-area projection and allows evaluating the overall quality of the result (Delvaux and Barth 2010).

Figure 6 represents the lower-hemisphere equal-area stereographic projections of the formal stress inversion of eight focal mechanism solutions of earthquakes occurred in Diyala city. The left panel is the result of applying the Rotational Optimization method, while the right panel is the result of the Rotational Optimization method. The selected focal planes are shown as great circles and associated slip lines as black dots with outward arrow. Stress inversion results are depicted by the orientation of the three principal stress axes, which are represented by a red dot surrounded by a circle for $\sigma_1$, a triangle for $\sigma_2$, and a square for $\sigma_3$. The related horizontal stress axes are represented by large blue arrow outside the stereogram for $S_H$ and red arrow for $S_h$. The orientations of the related moment stress axes are depicted by a small gray circle for the P-axis, a triangle for the N-axis, and a square for the T-axis. The directions of the horizontal stress axes are represented by the black bars on the periphery of the stereogram for the $S_H$ and white bars for $S_h$ for individual focal mechanisms. The small circle on the upper left corner of left panel shows the direction and type of the horizontal stress axes. The histograms to the lower left corner of the stereograms depict the distribution of the misfit angle F5 in the TENSOR program weighted arithmetically according to the magnitude for each case.

A quality ranking scheme of stress orientations determined from focal mechanisms was developed by Zoback

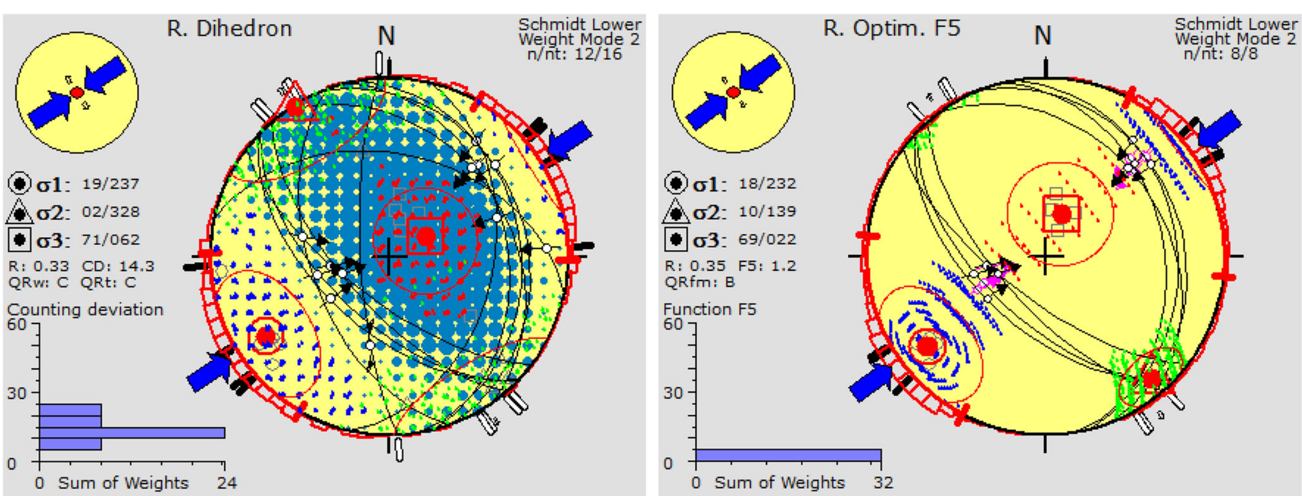


**Fig. 6** The results of formal stress inversion of eight focal mechanism solutions by the Improved Right Dihedron method (*left panel*) and the Rotational Optimization method (*right panel*). For more detail see the text

and Zoback (1989, 1991) and Zoback (1992) and updated by Sperner et al. (2003). Five qualities are used in ranking the data, which are between A and E, with A being the highest quality and E the lowest. The misfit angle is ≤12° for A quality, ≤20° for B quality, and ≤25° for C quality. The stress inversions eighth focal mechanism solutions of the study area were determined to be of B quality (QRfm in the right panel of Fig. 6).

The right panel of Fig. 6 shows the two solutions of fault in the study area, which is reverse fault. The fault plane solution is 60°/226° (dip angle and dip direction), while the axillary plane solution is 32°/023°. The attitudes of the principal stress axes (plunge angle and plunge direction) are: $\sigma_1 = 14°/217°$, $\sigma_2 = 10°/309°$ and $\sigma_3 = 72°/074°$.

## Conclusions

Diyala city is one of the most seismically active cities in Iraq. Depending on three seismic catalogs (EMSC, IRIS and IRSC), six seismic swarms were distinguished; these are: January 2005, September 2008, June 2009, August 2009, November 2013, and August 2014. Eight focal mechanism solutions were calculated from the GCMT catalog. The solutions indicate that the movement on faults in the study area is a reverse movement formed by compressional forces. In order to estimate the directions of the three principal stress axes that effect on faults in Diyala city, two methods were used; these are: the Improved Right Dihedron and Rotational Optimization. The fault plane solution is 60°/226°, while the auxiliary plane solution is 32°/023°. The attitudes of the principal stress axes are: $\sigma_1 = 14°/217°$, $\sigma_2 = 10°/309°$ and $\sigma_3 = 72°/074°$.

The seismic activity in Diyala city is due to the collision between the Arabian and Iranian plates. The study area has many faults, but the most active one in our opinion is represented by the northern part of Badra-Amarah fault. This fault extends from Mandali city in the northwest and passes Badra city, until it reaches Amarah city in the southeast. This fault is the most active fault in Iraq; and it represents the northeastern boundary between the folded and unfolded Zones. Additionally, there is another seismic active area located between Khanaqin and Qasr-e Shirin cites. We believe that these activities are related to a small fault with direction NW–SE located between these two cites. This fault was diagnosed by the satellite images. We highly recommend more seismic and geophysical studies in Diyala to shade more light on the seismotectonics of the region.

**Acknowledgments** Our acknowledgement goes to the Iranian Seismological Center (IRSC), the European-Mediterranean Seismological Centre (EMSC), the Incorporated Research Institutions for Seismology (IRIS), and the Global Centroid-Moment-Tensor (GCMT) Project for providing the earthquake parameters and focal mechanism solutions. We are also grateful to Dr. Delvaux and Sperner for their TENSOR program, and Wessel and Smith for the GMT software.

## References

Abdulnaby W, Mahdi H, Numan NMS, Al-Shukri H (2013) Seismotectonics of the Bitlis–Zagros Fold and Thrust Belt in Northern Iraq and surrounding regions from moment tensor analysis. Pure Appl Geophys. doi:10.1007/s00024-013-0688-4

Abdulnaby W, Mahdi H, Al-Shukri H, Numan NMS (2014) Stress patterns in Northern Iraq and surrounding regions from formal stress inversion of earthquake focal mechanism solutions. Pure Appl Geophys. doi:10.1007/s00024-014-0823-x

Abdulnaby W, Al-Mohmed R, Mahdi M (2015) Seismotectonic of Badra-Amarah Fault, Iraq-Iran border. IOSR J Appl Geol Geophys (IOSR-JAGG) 4(3):27–33

Alsinawi SA (1988) Historical seismicity of the Arab countries. In: Proceedings of the 3rd Arab seismological seminar-King Saud University, Riyadh, Saudi Arabia, vol 7, pp 11–33

Delvaux D (1993) The TENSOR program for paleostress reconstruction: examples from the east African and the Baikal rift zones. In: Terra abstracts. Abstract supplement no 1 to Terra Nova, vol 5, p 216

Delvaux D, Barth A (2010) African stress pattern from formal inversion of focal mechanism data. Implications for rifting dynamics. Tectonophysics 482:105–128

Delvaux D, Sperner B (2003) Stress tensor inversion from fault kinematic indicators and focal mechanism data: the TENSOR program. In: Nieuwland D (ed) New insights into structural interpretation and modelling, Special Publications, vol 212. Geological Society, London, pp 75–100

Dziewonski AM, Chou TA, Woodhouse JH (1981) Determination of earthquake source parameters from waveform data for studies of global and regional seismicity. J Geophys Res 86:2825–2852. doi:10.1029/JB086iB04p02825

Ekström G, Nettles M, Dziewonski AM (2012) The global CMT project 2004–2010: centroid-moment tensors for 13,017 earthquakes. Phys Earth Planet Inter 200–201:1–9. doi:10.1016/j.pepi.2012.04.002

Fouad SFA, Sissakian V (2011) Tectonic and structural evolution of the mesopotamian plain. Iraqi Bull Geol Min Spec Issue 4:33–46

Jassim SZ, Goff JC (2006) Geology of Iraq. Dolin, Prague and Moravian Museum, Brno, Czech Republic, p 341

Keilis-Borok VL, Knopoff L, Rotwain IM, Siderenko TM (1978) Bursts of seismicity as long term precursors of strong earthquakes. In: Proc. Conf. VI, methodology for identifying seismic gaps and soon to break gaps, 351–386

Michael AJ, Toksoz MN (1982) Earthquake swarms as a long-range precursor to large earthquakes in Turkey. Geophys J R Astr Soc. 68:459–476

Numan NMS (1997) A plate tectonic scenario for the Phanerozoic succession in Iraq. Iraqi Geol J 30:85–119

Numan NMS, Al-Azzawi N (1993) Structural and geotectonic interpretation of vergence directions of anticlines in the foreland folds of Iraq. Abahath Al-Yarmouk 2:57–73

Seber D, Vallve M, Sandvol E, Steer D, Barazangi M (1997) Middle east tectonics: applications of geographic information systems (GIS). GSA Today Publ Geol Soc Am 7(2):1–5

Sperner B, Müller B, Heidbach O, Delvaux D, Reinecker J, Fuchs K (2003) Tectonic stress in the Earth's crust: advances in the

World Stress Map project. In: Nieuwland DA (ed) New Insights into structural interpretation and modelling. Geological society special publication, no 212. Geological Society, London, pp 101–116

Zoback ML (1992) First and second-order patterns of stress in the lithosphere: the World Stress Map Project. J Geophys Res 97(B8):11703–11728

Zoback ML, Zoback MD (1989) Tectonic stress field of the conterminous United States. Mem Geol Soc Am. 172:523–553

Zoback MD, Zoback ML (1991) Tectonic stress field of North America and relative plate motions. In: Slemmons DB, Engdahl ER, Zoback MD, Blackwell DD (eds) Neotectonics of North America, pp 339–366